# PELLET INJECTION INTO ASDEX UPGRADE PLASMAS WITH IMPROVED SZENARIO FROM THE MAGNETIC HIGH-FIELD SIDE

P.T. Lang, K. Büchl, M. Kaufmann, R.S. Lang, V. Mertensr
H.W. Müller, J. Neuhauser, ASDEX Upgrade Team, NBI Team

IPP 1/304 Oktober 1996

MAX-PLANCK-INSTITUT FÜR PLASMAPHYSIK

85748 GARCHING BEI MÜNCHEN

MAX-PLANCK-INSTITUT FÜR PLASMAPHYSIK
GARCHING BEI MÜNCHEN

# PELLET INJECTION INTO ASDEX UPGRADE PLASMAS WITH IMPROVED SZENARIO FROM THE MAGNETIC HIGH-FIELD SIDE

P.T. Lang, K. Büchl, M. Kaufmann, R.S. Lang, V. Mertensr
H.W. Müller, J. Neuhauser, ASDEX Upgrade Team, NBI Team

IPP 1/304 Oktober 1996

*Die nachstehende Arbeit wurde im Rahmen des Vertrages zwischen dem Max-Planck-Institut für Plasmaphysik und der Europäischen Atomgemeinschaft über die Zusammenarbeit auf dem Gebiete der Plasmaphysik durchgeführt.*

# PELLET INJECTION INTO ASDEX UPGRADE PLASMAS WITH IMPROVED SZENARIO FROM THE MAGNETIC HIGH-FIELD SIDE

P. T. Lang, K. Büchl, M. Kaufmann, R.S. Lang, V. Mertens,
H.W. Müller, J. Neuhauser, ASDEX Upgrade Team, NBI Team

Max-Planck-Institut für Plasmaphysik
EURATOM Association
Boltzmannstr. 2, 85748 Garching, Germany

## ABSTRACT

High-efficiency tokamak plasma refuelling with cryogenic pellets injected from the magnetic high-field side is demonstrated. In this novel injection scheme, a blower gun was used to inject deuterium pellets (up to 130m/s at up to 17 Hz) through a guiding tube from the magnetic high-field side of the ASDEX Upgrade divertor tokamak. In contrast to standard low-field side injection, these experiments, performed in ELMy H-mode discharges, showed almost no rapid loss of particles and energy. Consequently, under identical starting conditions, the plasma refuelling efficiency was up to 4 times as large as for the standard injection scheme with virtually unchanged energy confinement. We believe that the large, nearly instantaneous particle losses in the standard scheme are mainly due to the toroidal drift force pushing deposited material towards the low-field side plasma edge and eventually out of the plasma column in the case of shallow pellet penetration. In contrast, for shallow high-field side injection, this drift is directed towards the plasma core and therefore enhances bulk fuelling. In this new scheme, a further benefit is derived from enhanced pellet shielding, and hence deeper pellet penetration, caused by the ablated material drifting in the same direction as the solid pellet in the case of high-field side injection.

## Table of Contents

Abstract.....1

Table of Contents.....2

1. Introduction.....3

2. Experimental setup.....4
   2.1 Ppellet injectors.....4
   2.2 Diagnostics.....5
   2.3 Operating conditions.....6

3. Results.....7
   3.1. Injection from the LFS.....7
   3.2. Injection from the HFS.....12

4. Discussion and Conclusion.....21

References.....23

# 1. INTRODUCTION

Controlled refuelling of deuterium (D) and tritium (T) into the burning plasma is a basic requirement for operation of a fusion reactor. In present tokamaks usually the density of the plasma is feedback controlled using valves for the injection of neutral gas into the vessel. Refering to gas consumption, this method shows low efficiency; only a small fraction of injected particles finally enters the plasma. Because of the low efficiency, gas puffing enforces a high T fuel reservoir and hence a high hazard potential. Future thermonuclear fusion reactors like ITER are proposed to operate at high density [1], requireing probabely too high particle fluxes to achieve necessary plasma densities.

A more adequate fuelling method may be the injection of solid pellets, which deposits the fuel in discharges with low heating power deep inside the plasma. However, experiments in various devices [2] have shown that in discharges with high heating power and especially in type-I ELMy H-mode plasmas with high edge temperatures the penetration depths of pellets are small and the high fuelling efficiency of this method can be lost. A common feature of all these previous pellet experiments is injection from the magnetic low-field side (LFS), i.e. from the torus outside, which is easily accessible. Due to unfavourable toroidal drift effects a large fraction of the deposited material is rapidly expelled from the plasma, resulting in significantly reduced fuelling efficiencies especially with shallow penetration. However, with injection from the magnetic high-field side (HFS), i.e. the torus inside, the same drift force should rapidly transport the deposited pellet material towards the plasma core and therefore even enhance the bulk plasma fuelling efficiency.

In order to clarify this question, experiments have been conducted in ASDEX Upgrade where pellets were injected from both sides into H-mode plasmas and fuelling efficiencies as well as pellet penetration depths were compared.

## 2. EXPERIMENTAL SETUP

### 2.1 Pellet injectors

Pellet injection is performed either with a centrifuge injector or a blower gun; a scetch of the setup is shown in figure 1. The centrifuge injects only from the LFS with the capability of varying the pellet velocity (240 to 1200 m/s) and/or mass (1.7 to 4.3 x $10^{20}$ particles) [3] in order to allow a variation of the deposition profile. Cubic pellets formed from pure hydrogen or deuterium were injected horizontally from the torus low-field side at the midplane of the standard single-null plasma configuration, tilted $11^{o}$ from the radial direction. Injection can be performed at repetition rates of up to 80 Hz, either as pre-programmed sequences or feedback-controlled via the ASDEX Upgrade plasma discharge control system [4] to achieve density control by the pellets.

The blower gun injects $D_2$ pellets containing 3 x $10^{20}$ particles, accelerated by $H_2$ gas flow of up to 130 m/s at repetition rates of up

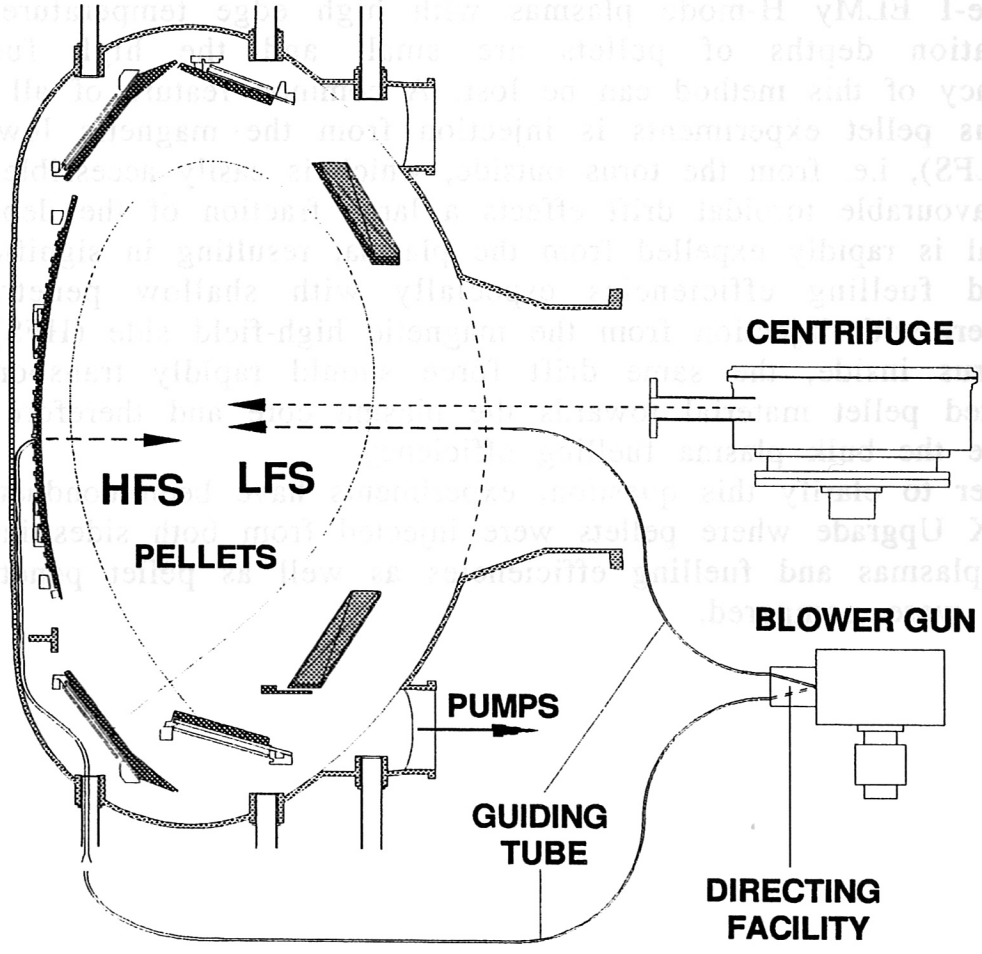


*Figure 1: Cross-section of the ASDEX Upgrade divertor tokamak. Pellet injection is performed by the centrifuge or via guiding tubes by the blower gun.*

to 17 Hz. Pellets are delivered via guiding tubes optionally from the magnetic low or high-field side. Switching from one track to the other is possible within 60 ms. An example of a pellet injected from the HFS into the plasma by means of the blower gun via the guiding tube is shown in figure 2.

## 2.2 Diagnostics

Pellet ablation and penetration are monitored by several CCD cameras (time resolution 10 ms) and photodiodes (max. temporal resolution 2μs) measuring the $H_\alpha/D_\alpha$ (Balmer alpha, n=3 → n=2 transition; centred at 656.5/656.1nm) light emission. A pellet light barrier detector array, mounted at the centrifuge exit to determine the exact flight path of the pellet, together with the pellet CCD picture, allows one to determine whether the pellet enters the discharge as a whole or split into several pieces. Due to the lack of a pellet mass detector, the real pellet mass was unknown.

Bird´s-eye-view video pictures showing the ablation zone of the pellets are used to evaluate the pellet penetration depths. Numerous diagnostics were used to study the plasma behaviour [5]. For example, line-averaged electron densities were measured by an eight-chord DCN laser interferometer; the plasma particle inventory and Abel-inverted density profiles were calculated by means of these data. For checking and, in cases where fringes were missed, correcting the interferometer data, three bremsstrahlung detection systems are available. A microwave reflectometry system was applied for density measurements at the plasma edge. Langmuir probes flush-mounted in the divertor target plates and a thermographic system provided information on particle and heat flux into the divertor. Several manometers, placed throughout the vessel, measured the neutral gas pressure. Electron temperatures were determined by Thomson scattering and electron cyclotron emission (ECE). Furthermore, data provided by the electromagnetic probes were used during this analysis.

The measured increase of the number of particles in the target plasma (1-2 ms after ablation) divided by the pellet mass is defined as the fuelling efficiency $\varepsilon_f$. To calculate $\varepsilon_f$ we used the maximum pellet mass found in testbed shots at the exit of the injectors, including the guiding tubes. Thus, the calculated values systematically underestimate the fuelling efficiencies. In the case of HFS injection, mass losses enhanced with respect to testbed values can occur in the experiment due to coupling of inner and outer guiding tubes. As these losses may strongly differ for different pellets, they cause strong scatter of $\varepsilon_f$ in the case of HFS injection.

## 2.3 Operating conditions

For all pellet injection experiments, ASDEX Upgrade was operated in a lower single-null divertor configuration ($R_0$=1.65m, a=0.5m, $\kappa$=1.7, $V_{Plasma}$=13$m^3$). Wall elements in contact with the plasma are covered by graphite tiles, the divertor target plates were tungsten-coated during this experimental campaign, and the vessel is routinely boronized. For plasma heating, besides ohmic heating, a four-beam NI injector able to produce a ´staircase´ power waveform, was applied. Use was made of the different H-mode power thresholds for the two directions of the ion $\nabla B$ drift [6] to change the confinement regime for a dedicated heating power $P_{heat}$ at a given magnetic configuration by changing the sign of $B_T$.

Several calibrated valves mounted at the vessel midplane are used for gas puffing, and turbomolecular pumps with a pumping speed of 14 $m^3/s$ for D control particle exhaust.

The experiments described here were carried out in D with $I_P$ = 0.8 - 1.2 MA, $|B_t|$ = 1.7 - 2.5 T, $q_{95}$ = 2.7 - 4.2 and additional $H^0/D^0$-beam injection heating of up to 7/10 MW.

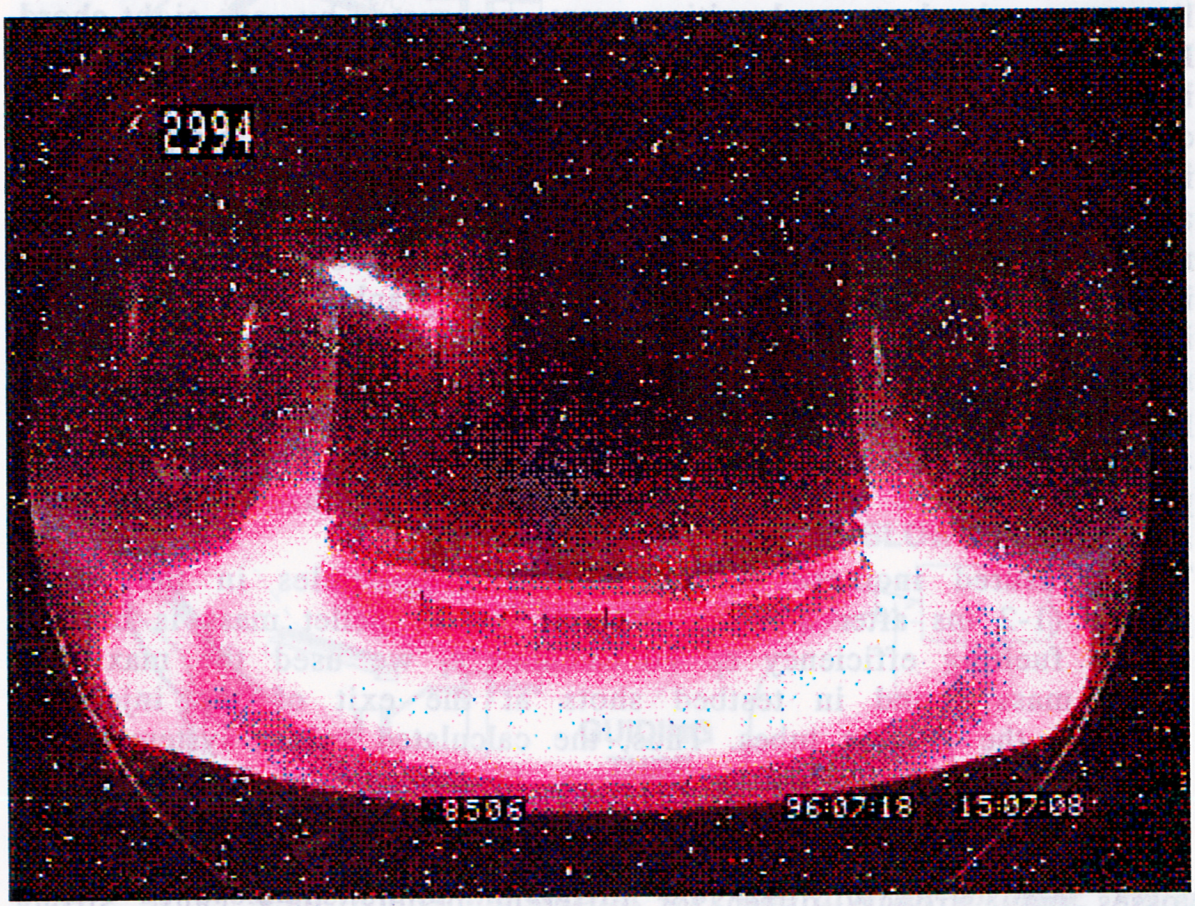


*Figure 2: Wide-angle view into the ASDEX Upgrade tokamak in the light of the $H_\alpha/D_\alpha$ emission line. The ablation radiation emitted from a pellet entering the plasma from the HFS can be clearly seen.*

## 3. RESULTS

The experiments reported were performed with the intention to study the behaviour of pellet-refuelled discharges in the H-mode regime with improved injection scenario from the HFS. Experimental results are compared to observations already reported. For LFS injection, the pellet efficiency was found to decrease with increasing heating power and especially when the type-I ELMy H-mode regime is entered.

### 3.1. Injection from the LFS

Fuelling efficiencies close to unity and accordingly a strong influence on the discharge behaviour were found for pellet injection into ohmic plasmas ($P_{OH} \approx 1MW$). Comparing the dynamic ablation profile obtained from the $H_\alpha/D_\alpha$ signal [7,8] with the increment of the radial density profile a few ms after the ablation process showed nearly all pellet material to be confined just where it had been deposited. Successful density buildup beyond the density limit achieved by gas puffing was possible by repetitive injection of pellets at an adequate rate. Pellet refuelling can yield strong peaking of the density profile, even in cases of pellet penetration less than half the minor plasma radius, clearly causing a change of the particle transport. Further, pellet refuelling of ohmic discharges can also yield better confinement both for the energy and the particles. This behaviour can be interpreted as restoring the situation in the linear part of the $\tau_E / \overline{n_e}$ curve by the pellets up to $\overline{n_e}$ values where the normal gas puff data show already saturation of $\tau_E$, a detailed discussion of this question has already been given in [9].

It turned out, however, the favourable behaviour observed for ohmic heating only ($P_{NI}=0$) is lost with additional heating power applied by neutral beam injection. This is illustrated in Fig.3, where experimental values of $\varepsilon_f$ are plotted versus the applied additional heating power, triangles indicating pellets injected during L-mode phases (or in OH discharges), circles injection in H-mode plasmas. Appropriate experiments were performed by injecting sequences of a few pellets at a low repetition rate, not changing the target plasma too strongly by the pellets themselves, into discharges heated with varying neutral beam heating power. The solid line in Fig.3, representing the fuelling efficiency achieved under optimum conditions (most likely nearly "perfect" pellets), shows the strong fuelling efficiency degradation with increasing heating power. Thus, in our experiment, a maximum fuelling efficiency of only 0.3 could be achieved with about 7MW of NI heating power. The degradation of $\varepsilon_f$ with increasing additional heating power has already been reported for many other

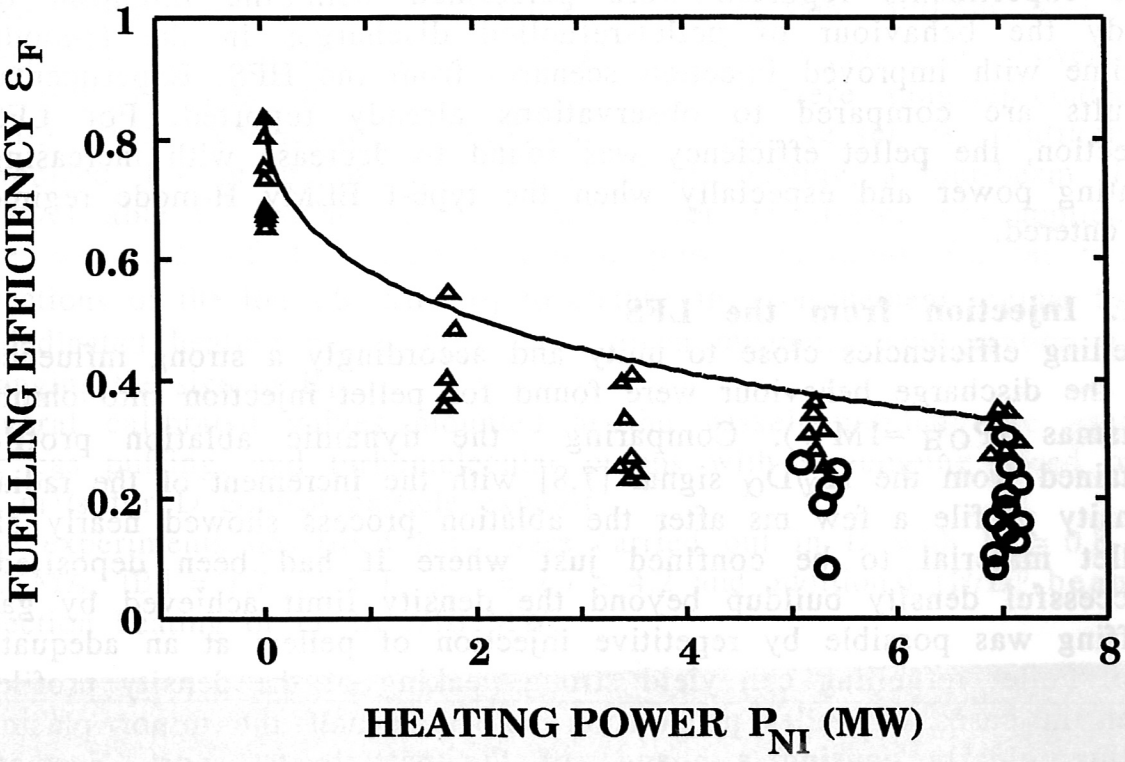


*Fig. 3: Pellet fuelling efficiency versus applied additional heating power, $\varepsilon_f$ is calculated assuming nominal pellet masses. Triangles: pellet injection during L-mode phases or into ohmic plasmas; circles: H-mode target plasmas; solid line: limiting curve of maximum fuelling efficiency, representing $\varepsilon_f$ ($P_{NI}$) obtained for ideal conditions (e.g. nominal pellet mass).*

*Fig. 4(right): a,b) Video frames taken during pellet injection into NI heated plasmas ($B_t$=2.5T; $P_{NI}$ = 7.3MW in a); $P_{NI}$ = 3.7MW in b)), showing expelled material (indicated by luminescent region) concentrated within a tube of few cm in diameter following magnetic field lines. Changing the toroidal field direction ( $\nabla B$ drift upwards in a); $\nabla B$ drift downwards in b)) accordingly alters the helicity of field lines. c) No similar structures are present in a colder pure ohmic discharge. In this case the video frame shows only the ablation along the pellet path.*

Pellet ablation
Expelled material
c
b
a

tokamaks [10-15]. According to investigations performed on JET and TFTR [16], but also to analysis of data from ASDEX, the $\varepsilon_f$ degradation is accompanied by a growing shift of the effective deposition profile towards the separatrix. With increasing $P_{heat}$, a growing discrepancy between the dynamical ablation rate profile, reconstructed by mapping the $H_\alpha/D_\alpha$ emission from the ablating pellet onto the radial location of the pellet trajectory, and the effective ablation rate profile, determined from the change in the density profile (1-2 ms after the ablation), was observed.

For pellets injected into strongly heated plasmas ($P_{NI} > 5MW$), there is an immediate (temporal resolution about 1ms) onset of strong particle flux following pellet injection, as detected by the reflectometer and by the Langmuir probes mounted in the divertor plates. From the neutral gas gauge signals also the amount of particles expelled by this pellet-induced flux was confirmed to be close to the pellets´ initial mass.

Video observations of the area near the pellet injection port, like in Fig.4, show the expelled material not to be isotropically distributed but still concentrated in a small tube at the plasma edge (∅ few cm) toroidally following the magnetic field lines. Mapping the observed luminiscent structures onto the magnetic field structure confirmed also sticking of the plasmoid to the field lines. Fig.4a and 4b, taken during pellet injection into discharges with reversed toroidal field direction ($\nabla B$ drift upwards in Fig.4a, downwards in Fig.4b) clearly visualizes the according change of field line helicity. A test observation performed for a colder ohmic plasma (Fig.4c) only showed the ablation trace along the pellet path; no structures corresponding to those observed in pellet injection into strongly heated plasmas were found.

For our efforts made on achieving efficient refuelling for density rampup or even controlling for additionally heated plasmas in the high confinement regime, more problems than the power degradation were enfaced. When injecting slow and small pellets during type I ELMy phases, a further reduction beyond the $\varepsilon_f$ degradation with $P_{NI}$ takes place. The H-mode degradation of the fuelling efficiency was found to show strong dependence on the penetration depths of the injected pellets. When slow and small pellets were injected, only a small fuelling efficiency could be found. For deeper penetration, the L-mode values are recovered. This behaviour is attributed to the release of ELMs by the pellet and discussed in detail in [17].

Although the efficiency of pellet refuelling is rather limited for LFS injection of ELMy H-modes, high repetition rates allow for a density control on a level not acessible by gas puffing. This is demonstrated in

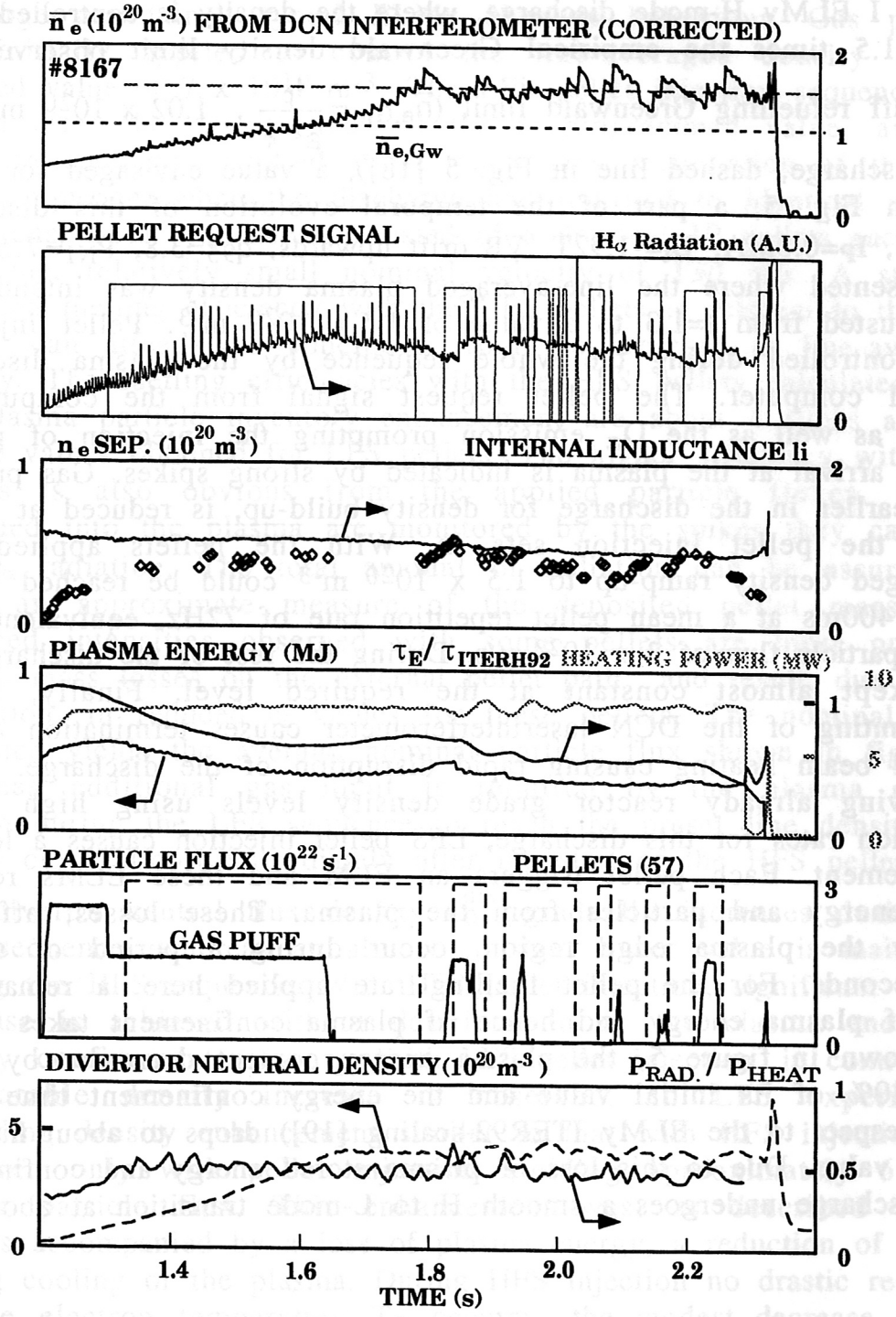


*Fig. 5 Density ramp-up and control by pellet refuelling. The line-averaged density (upper trace) is adjusted to an envisaged value of $1.5x10^{20}$ $m^{-3}$ by pellet injection (indicated by spikes in the $D\alpha$ signal, middle trace), controlled by the ASDEX Upgrade plasma discharge controlling computer. This realizes density control at a level 1.5 times the empirical density limit observed for gas puff refuelling, a value envisaged for ITER.*

a type I ELMy H-mode discharge, where the density is controlled on a level 1.5 times the empirical Greenwald density limit observed for gas puff refuelling Greenwald limit ($\bar{n}_{e,Gw} = \frac{I_p}{a^2 \pi}$, $1.02 \times 10^{20}$ $m^{-3}$ for this discharge, dashed line in Fig. 5 [18]), a value envisaged for ITER [1]. In Fig. 5, a part of the temporal evolution of this discharge (#8167, $I_P$=0.8MA, $B_t$=-1.92T, $\nabla B$ drift upwards, $q_{95}$=3.8, $P_{NI}$=7.5MW) is presented where the line-averaged plasma density was intended to be adjusted from t=1.3 to a value of $1.5 \times 10^{20}$ $m^{-3}$. Pellet injection was controlled during the whole sequence by the plasma discharge control computer. The pellet request signal from the computer is shown as well as the $D_\alpha$ emission prompting the injection of pellets whose arrival at the plasma is indicated by strong spikes. Gas puffing, used earlier in the discharge for density build-up, is reduced at t=1.3s when the pellet injection sets in. With the pellets applied, the envisaged density ramp-up to $1.5 \times 10^{20}$ $m^{-3}$ could be reached within about 400ms at a mean pellet repetition rate of 72Hz, equivalent to a mean particle flux of $3 \times 10^{22}$ at/s. During the rest of the discharge, $\overline{n_e}$ was kept almost constant at the required level. Finally, fringe miscounting of the DCN laserinterferometer causes termination of the neutral beam heating causing rapid disruption of the discharge.
Achieving already reactor grade density levels using high pellet repetition rates for this discharge, LFS pellet injection causes a loss of confinement. Each pellet triggers an ELM and these ELMs remove both energy and particles from the plasma. These losses, affecting mainly the plasma edge region, occur during a period of a few milliseconds. For the pellet fuelling rate applied here, a remarkably loss of plasma energy and hence of plasma confinement takes place. As shown in figure 5, the plasma energy content decreases by more than 40% of its initial value and the energy confinement time (here with respect to the ELMy ITER92-scaling [19]) drops to about half the initial value. Due to this loss of plasma stored energy and confinement the discharge undergoes a smooth H to L-mode transition at about 1.9 s.

### 3.2. Injection from the HFS

To demonstrate the enhanced refuelling performance of the HFS pellet injection scheme, LFS and HFS pellets were injected into the same plasma discharge under practically identical conditions. Figure 6 shows the temporal evolution of such a discharge ($I_P$ = 0.8 MA, $B_t$ = -1.9 T, $q_{95}$ = 3.6, $P_{NI}$ = 7.5 MW). During the whole sequence the

discharge maintained type-I ELMy H-mode behaviour. Gas puffing was initially applied to control the line-averaged density at the required value of 7 x $10^{19}$ $m^{-3}$. The LFS pellet injection sequence was started after the density reached the preprogrammed value, and the HFS sequence was applied about 0.5 s after termination of the LFS pellet sequence, when the discharge had returned to identical starting conditions. Both sequences consisted of a nominal 10 pellets each with the same, relatively small nominal velocity of 130 m/s. A strongly enhanced fuelling efficiency with the HFS pellets in relation to the LFS pellets can already be concluded from the increase in line-averaged density. The fuelling efficiencies with the HFS pellets calculated from the plasma particle inventory enhancement are about 4 times as high as the values obtained for LFS pellets. The higher efficiency with HFS pellets is also obvious from the applied particle fluxes. Pellets launched into the plasma are monitored by the spikes they cause in the $D_\alpha$ radiation. The total amount of radiation can be assumed to yield an approximate measure of the deposited pellet mass [20]. Reduced intensities observed with some pellets are most probably due to mass losses on the external pellet path and result, due to our definition, in reduced $\varepsilon_f$ values for these pellets. The nominal pellet sequence yields the average nominal particle flux shown in figure 6. Whereas additional gas input is required by the plasma control system during the LFS sequence to reach the preset line density, gas valves close almost immediately after the start of the HFS pellet train. The divertor neutral flux density $\Gamma_0^{div}$ gradually increases during the LFS sequence, whereas an almost constant lower value is maintained during the HFS sequence. With HFS pellet injection, significant density increase is achieved without deterioration of the plasma energy or energy confinement time $\tau_E$. With LFS pellet injection, in contrast, no comparable density increase is observed. In LFS experiments, according density enhancement similar to that with HFS injection was achieved only with pellet injection yielding approximately 6 times higher particle flux. This enhancement was, as described before, always accompanied by a loss of plasma energy, a reduction of $\tau_E$ and strong cooling of the plasma. During HFS injection no drastic reduction of the electron temperature $T_e$ occurs; the modest decrease of $T_{e0}$ shown in figure 6 is due to the density increase since the stored energy is not altered.

In addition to the direct comparison between LFS and HFS injection in the same discharge, a series of pellet injections from the HFS was performed under various plasma conditions. Figure 7 shows $\varepsilon_f$ values for different $P_{NI}$. For $P_{NI}$ > 5MW HFS pellets (filled symbols) showed efficiencies enhanced by up to four times that with LFS pellets (open

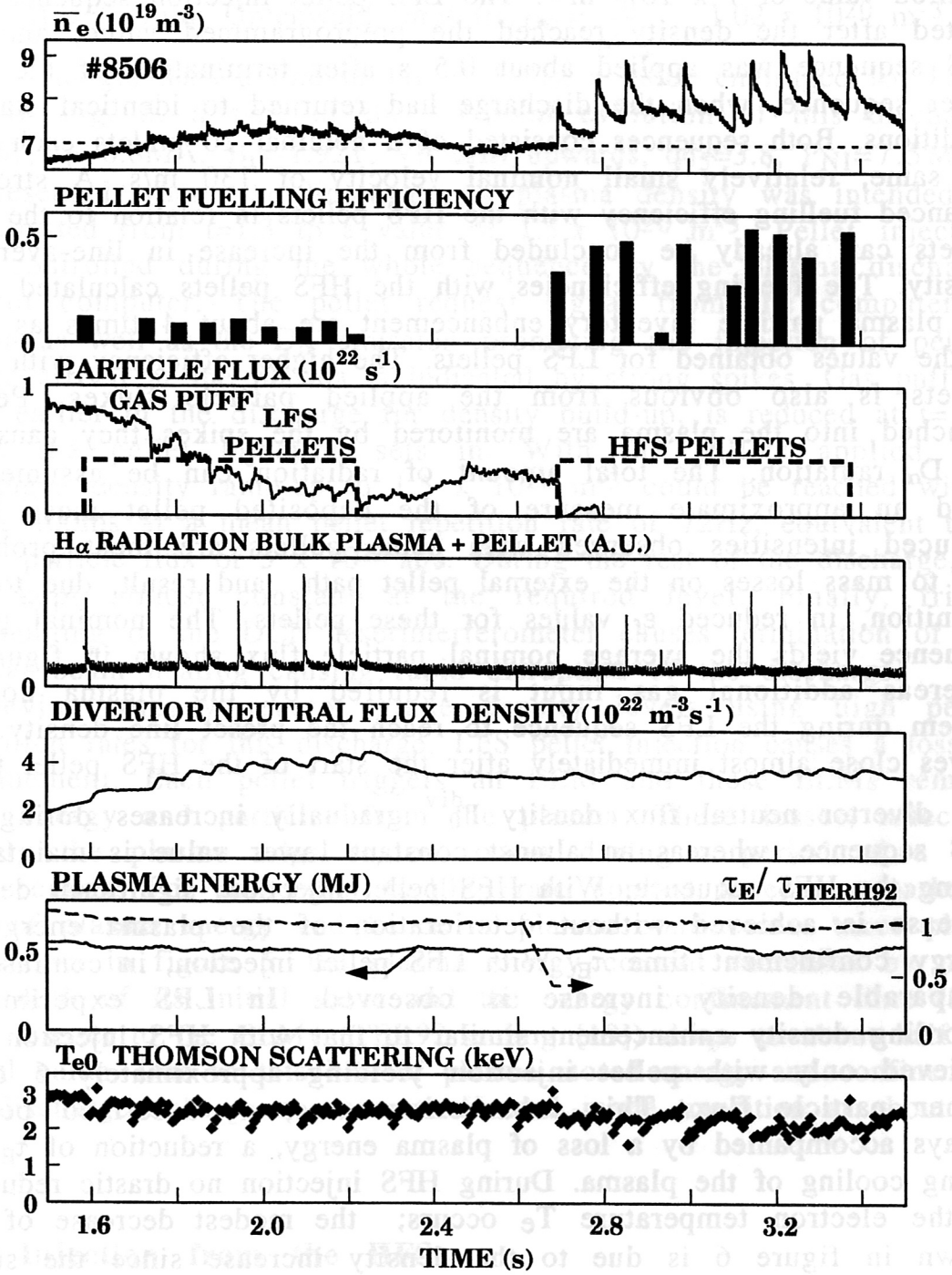


*Figure 6: Temporal evolution of a discharge with LFS and HFS pellet injection applied under identical pellets and plasma starting conditions.*

symbols). With increasing $P_{NI}$ and plasma temperature, HFS pellets show no significant power degradation of $\varepsilon_f$. Even at the highest heating powers applied almost the same efficiencies are achieved as in ohmic plasmas. As already mentioned, the strong scatter of $\varepsilon_f$ values is most probably an artefact caused by external pellet mass losses. This conclusion is further supported by the fact that reduced $\varepsilon_f$ values were always accompanied by reduced ablation radiation. With the ablation radiation being assumed to be a good measure of the pellet mass [20], accordingly corrected $\varepsilon_f$ values show a scatter reduced to ±10 % of the optimum value of ≈0.7. In contrast, only $\varepsilon_f <$ 0.4 was found for $P_{NI} >$ 5 MW with fast (1200 m/s) LFS pellets penetrating deep into the plasma; in the case of shallow penetration into type-I ELMy H-mode plasmas $\varepsilon_f$ was even restricted to values below 0.2 (see figure3). Comparable conditions yielded the same result in the case of LFS pellet injection with the blower gun, as shown in figure 7.

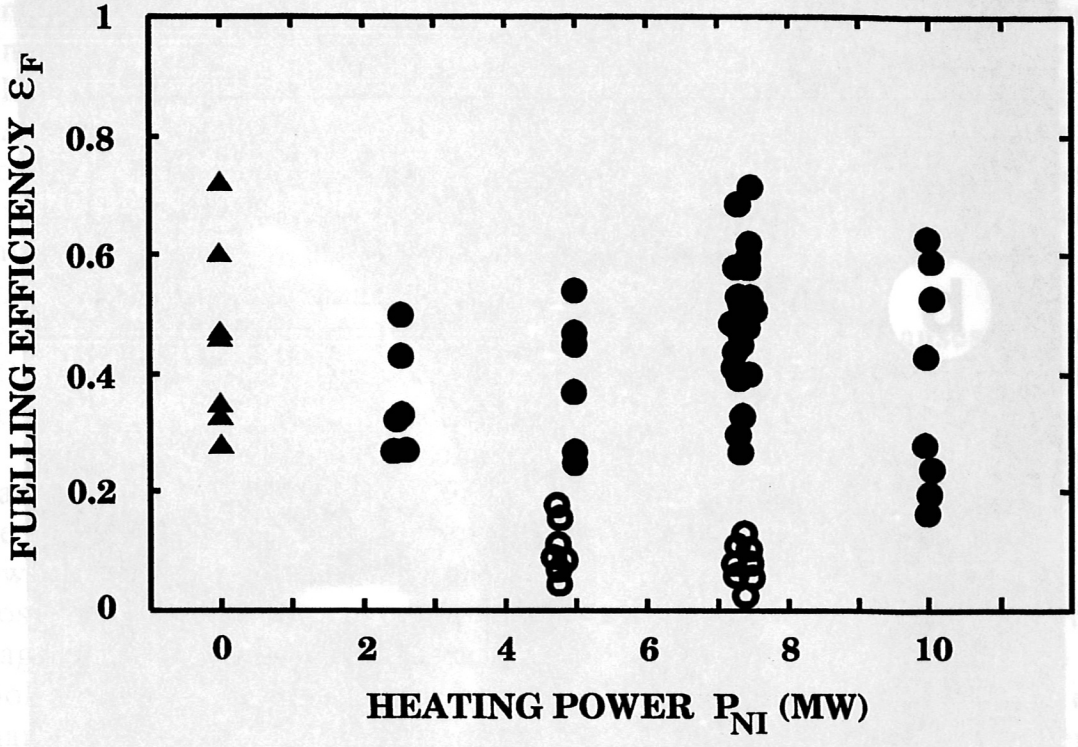


*Figure 7: Fuelling efficiency calculated on the assumption of maximum pellet masses versus additional heating power for LFS (open symbols) and HFS (filled symbols) pellets injected with the blower gun. Triangles: pellets into ohmic or L-mode plasmas; circles: H-mode target plasmas. The maximal pellet mass is that found in a similar, but not identical laboratory experiment.*

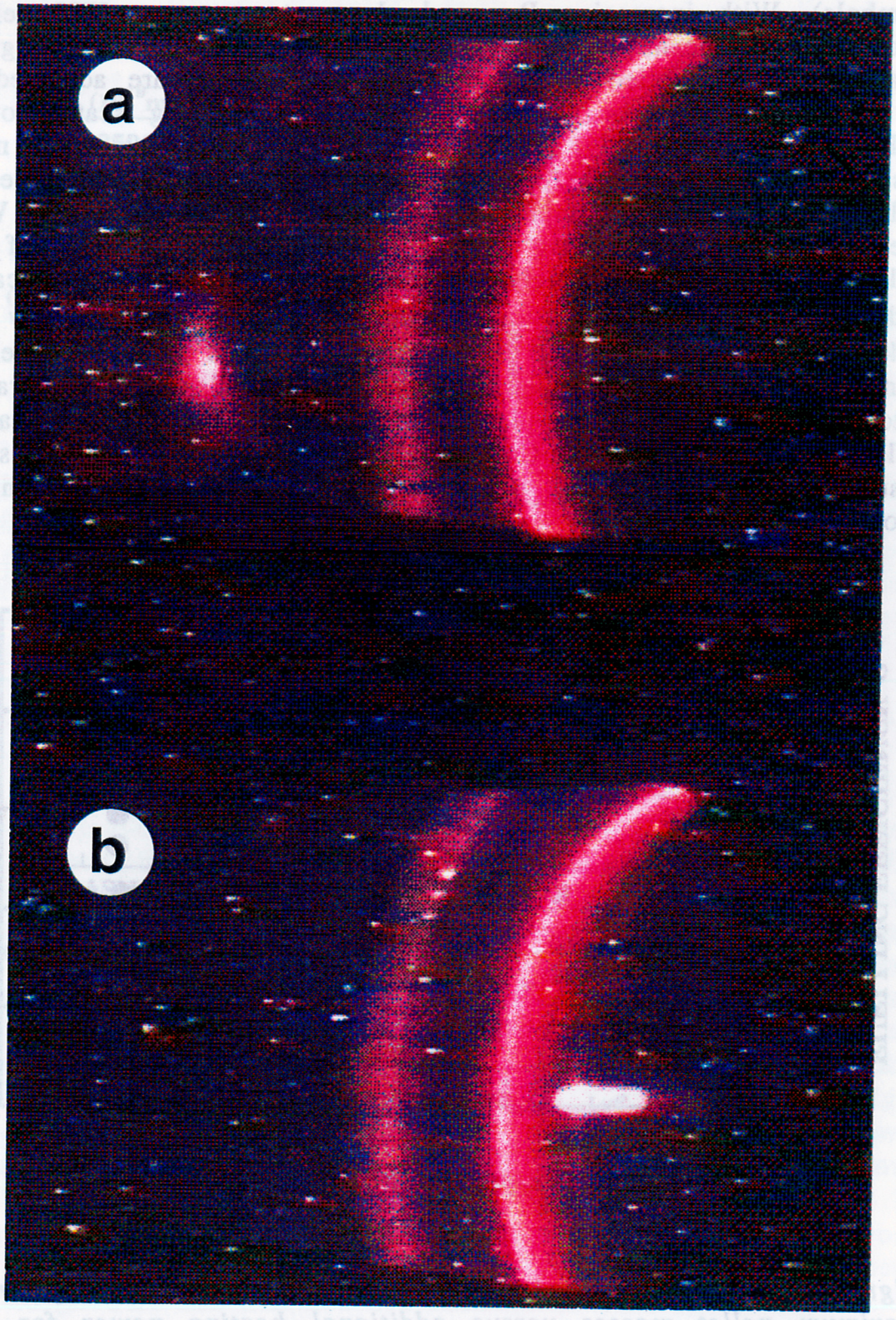


*Figure 8: Bird´s-eye-view pictures of pellet ablation traces recorded with a CCD camera for a) 6th LFS pellet and for b) 5th HFS pellet of figure 6. Inner (right) and outer (left) divertor strike points can be seen in the background.*

A further benefit of the HFS launch becomes obvious from video observations of the pellet path as shown in figure 8 for the same discharge as in figure 6. There is a striking difference in the pellet penetration depths $\Delta$ and ablation traces between LFS (a) and HFS pellets (b) . Whereas LFS penetration is rather low ($\Delta \approx 8$ cm in figure 8a), significantly deeper penetration ($\Delta \approx 19$ cm in figure 8b) is found with HFS pellets. This strong difference cannot be wholly attributed to different local target plasma conditions or different flux tube spacings (Shafranov shift); we estimate that these effects yield an enhancement of $\Delta$ with HFS pellets less than 1.6 times as large as the LFS values. Whereas LFS pellet penetration depths are in agreement with published ablation scalings, HFS pellets were found to penetrate considerably deeper into the plasma. We calculate $\Delta$ 6 - 9 cm for the LFS and $\Delta$ 9 - 14 cm for the HFS pellets, using an empirical scaling [21] obtained from the analysis of more than 100 previous LFS pellet injections into different ASDEX Upgrade discharges. The improved pellet penetration for HFS pellets can also be visualized when comparing to data obtained in a multimachine study regarding pellet penetration depths. In figure 9 penetration depths obtained for the pellets shown in figure 8 are plotted together with the data of the IPADBASE regression analysis [22]. Whereas LFS penetration is in the vicinity of the dataset, containing only results of LFS pellet injection experiments, HFS penetration shows enhanced pellet penetration. Thus, obviously, an additional shielding mechanism must be responsible for the enhanced $\Delta$ of HFS pellets.

Deeper penetration of HFS pellets obviously also causes growing influence on the plasmas central region. This is clearly indicated by the influence of pellet injection on the sawteeth behaviour, as shown in figure 10. Whereas no change in the behaviour of the sawtooth crashes is caused by the LFS pellets, identical pellets injected from the HFS alters the sawtooth behaviour drastically. Besides the sawtooth crashes occuring anyhow, events are observed which are most probably also sawteeth, triggered by the pellets. As the SXR diagnostics used for sawtooth identification is sensitive also to the cooling of the edge plasma by the pellet, the behaviour of the edge channel is somewhat disguised by the direct pellet effect. The central chord, however, indicates a pellet induced event showing a signature very similar to that of a sawtooth crash.

Like LFS injection, pellets injected from the HFS into an H-mode plasma trigger ELMs, as shown in figure 11. However, the corresponding direct pellet particle loss is obviously strongly reduced because of the deeper penetration of the frozen pellet itself and the

additional drift of ablated and ionized pellet material towards the plasma core and hence out of the ELM affected edge region.

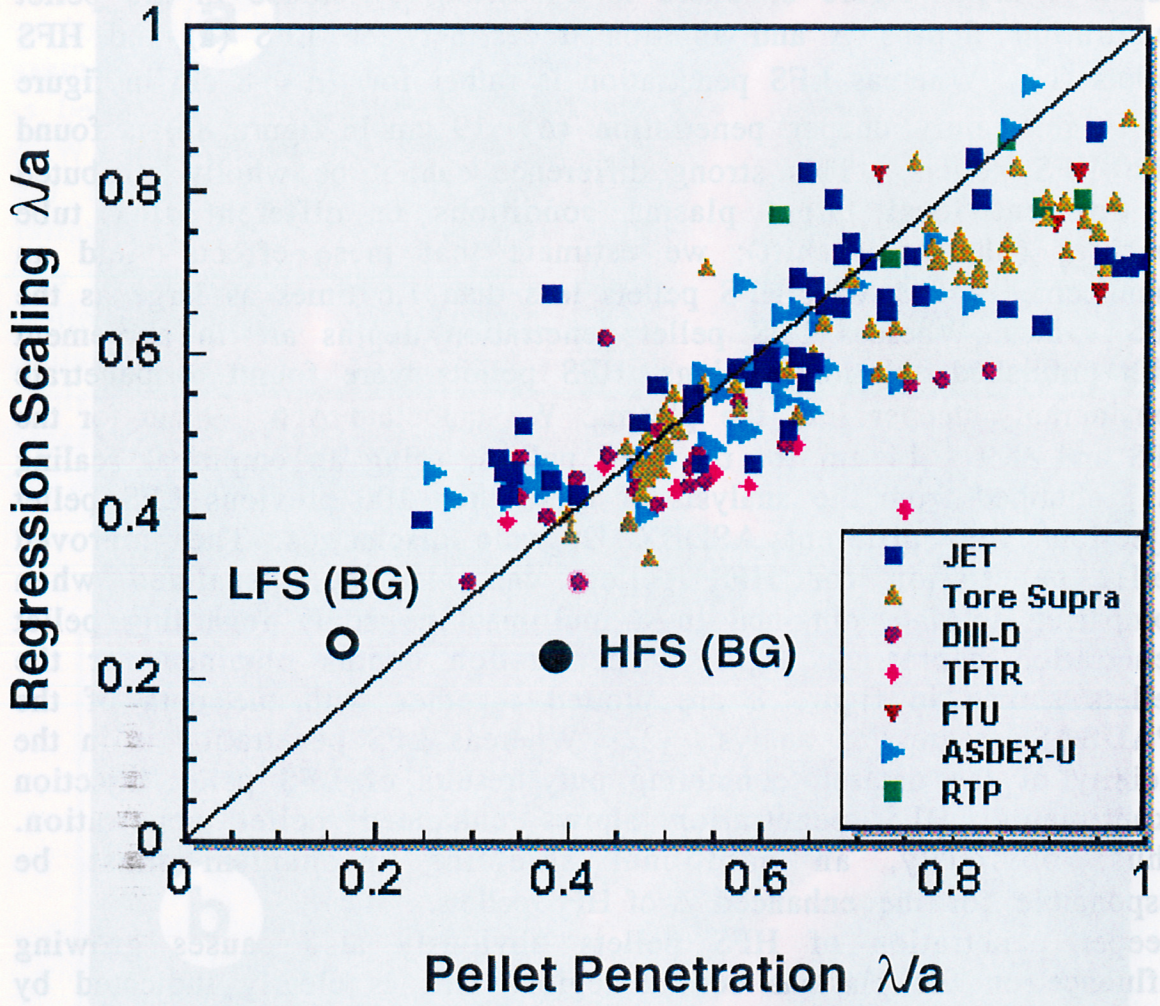


*Figure 9: Pellet penetration depths for the pellets shown in figure 8 compared with data of the IPADBASE multimachine regression analysis. Database contains results of pellet injection experiments from the LFS only.*

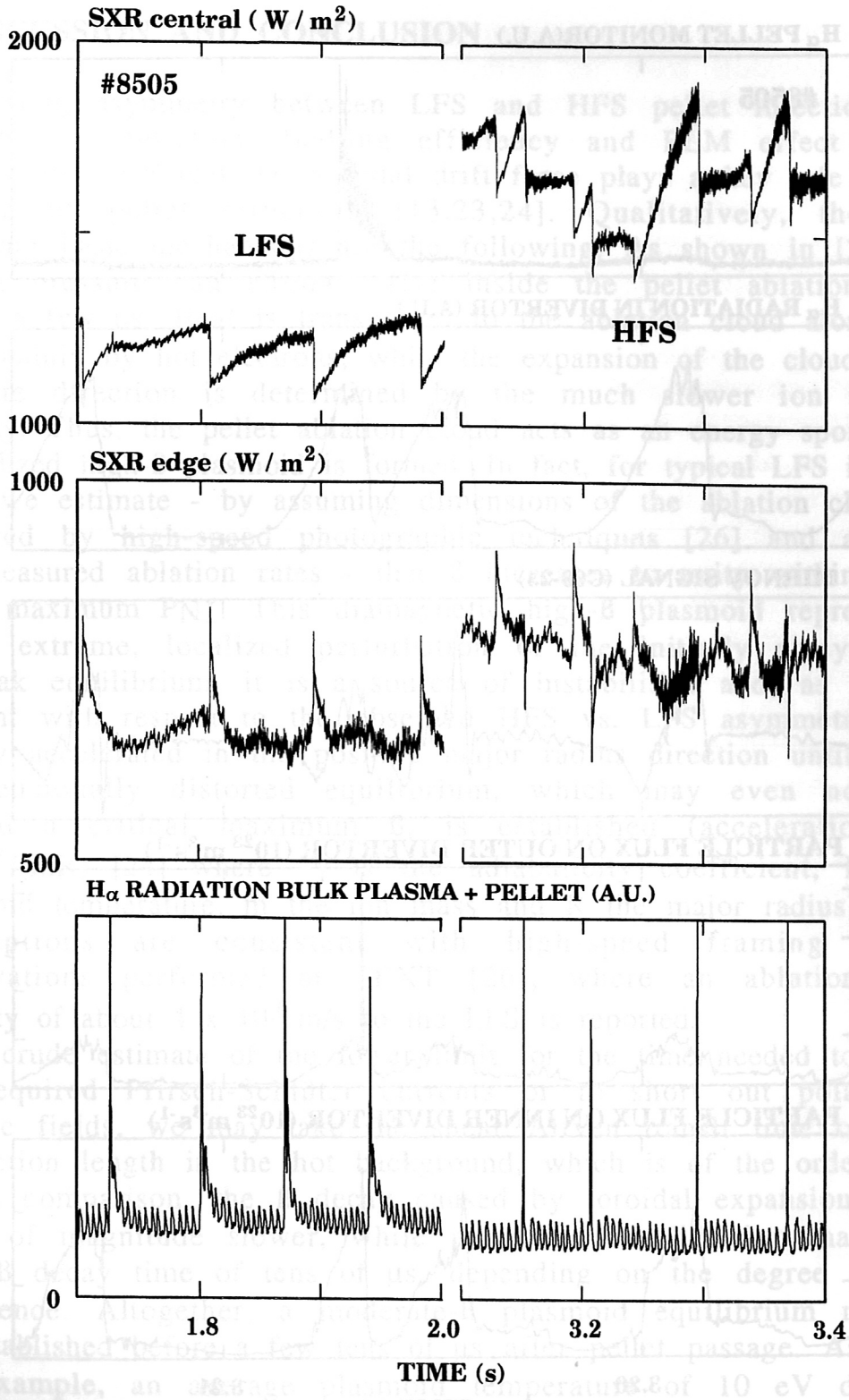


*Figure 10: Influence of the pellet injection on the sawteeth behaviour. Whereas for the case of LFS pellet injection (left) the sawtooth behaviour stays unchanged, HFS pellet injection alters the behaviour. Events very similar a sawtooth crash are triggered by each pellet injected from the HFS (right).*

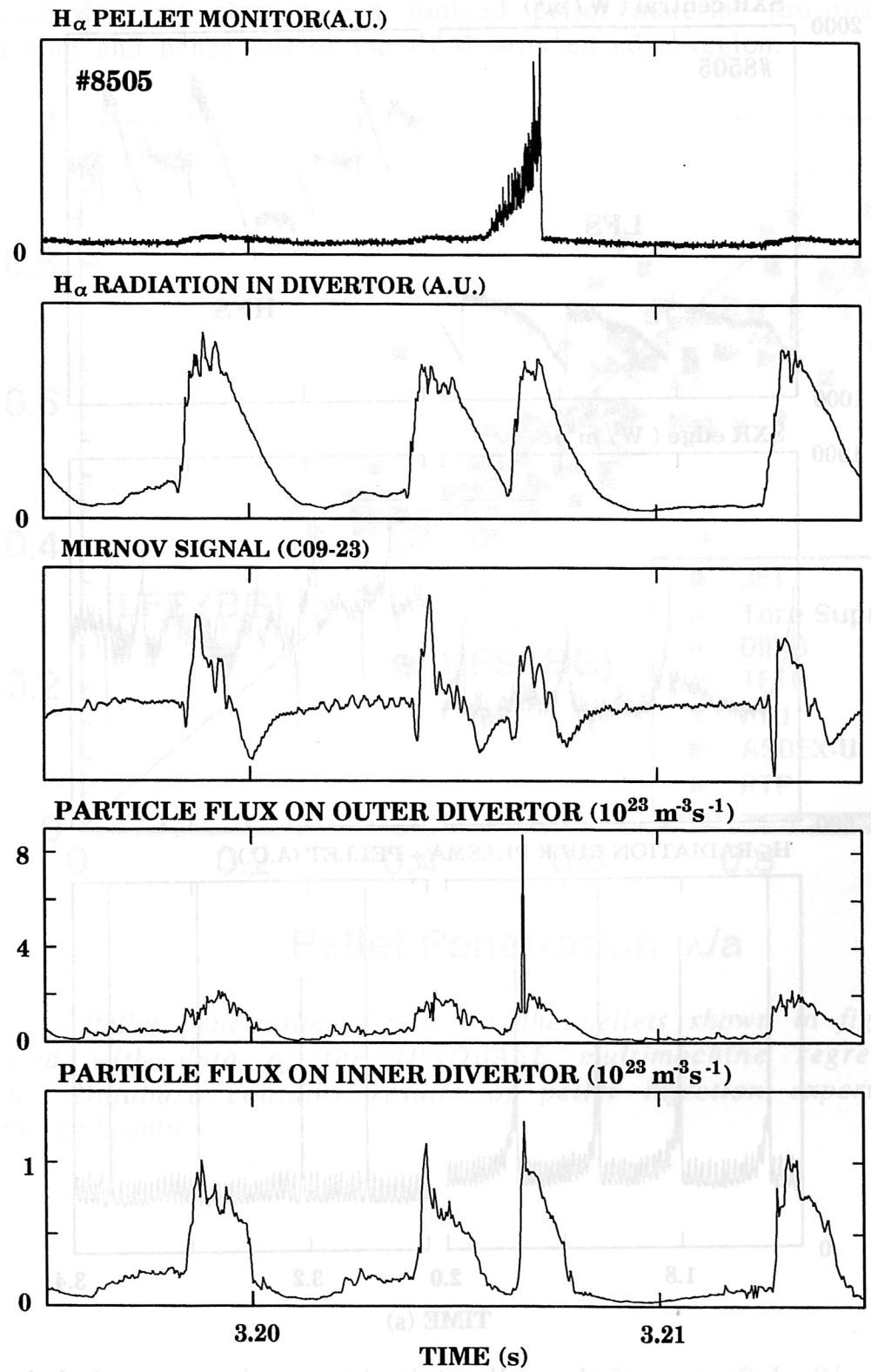


*Figure 11: Pellet injection from the HFS into a type-I ELMy H-mode discharge triggers an event showing the typical signature of an ELM. MHD activity as well as particle flux to the divertor caused by the pellet induced ELM are almost identical as for a regular ELM.*

## 4. DISCUSSION AND CONCLUSION

The strong asymmetry between LFS and HFS pellet injection with respect to penetration, fuelling efficiency and ELM effect clearly supports the idea that the toroidal drift force plays a key role for the success of pellet refuelling [13,23,24]. Qualitatively, the most important basic mechanisms are the following: As shown in [25], the plasma pressure can strongly rise inside the pellet ablation cloud within a few μs. Heat is transported to the ablation cloud along field lines mainly by hot electrons, while the expansion of the cloud in the opposite direction is determined by the much slower ion acoustic velocity. Thus, the pellet ablation cloud acts as an energy sponge and a localized high-ß plasmoid is formed. In fact, for typical LFS injection cases we estimate - by assuming dimensions of the ablation clouds as observed by high-speed photographic techniques [26] and adopting our measured ablation rates - that ß increases to unity within a few μs at maximum $P_{NI}$. This diamagnetic high-ß plasmoid represents a rather extreme, localized perturbation of the initially axisymmetric tokamak equilibrium, it is a source of instabilities and, as the key element with respect to the observed HFS vs. LFS asymmetry, it is rapidly accelerated in the positive major radius direction until a new 3-dimensionally distorted equilibrium, which may even not exist beyond a critical maximum ß, is established (acceleration $a = 4\gamma kT^*/(mR)$ [24] where $\gamma$ is the adiabaticity coefficient, $kT^*$ the plasmoid temperature, m the ion mass and R the major radius). These assumptions are consistent with high-speed framing camera observations performed at TEXT [26], where an ablation cloud velocity of about $4 \times 10^3$ m/s to the LFS is reported.

As a crude estimate of the lower limit for the time needed to set up the required Pfirsch-Schlüter currents or to short out polarization electric fields, we may take the shear Alfven transit time over one connection length in the hot background, which is of the order of 10 μs. In comparison, the ß decay caused by toroidal expansion is one order of magnitude slower, while perpendicular diffusion may result in a ß decay time of tens of μs, depending on the degree of local turbulence. Altogether, a moderate-ß plasmoid equilibrium may not be established before a few tens of μs after pellet passage. Assuming, for example, an average plasmoid temperature of 10 eV during a non-equilibrium phase of 20 μs for high $P_{NI}$, the plasmoid would be captured only after a major radius displacement of about 30 cm, this being of the order of typical pellet penetration depths.

This model provides a rather natural explanation of our experimental results: With LFS injection, part of the plasmoid nucleus may be

quickly lost, while the remaining pellet ablation halo is captured some distance downhill from its birthplace. A strong variation of $\varepsilon_f$ with plasma and pellet parameters is expected and observed. In contrast, even with shallow HFS injection, the drift force (and pellet mass inertia) is directed into the plasma, and (with ELM triggering neglected) nearly perfect absorption is to be expected rather independently of the system parameters, as observed. Even the enhanced pellet shielding and penetration are qualitatively understood since some earlier ablated material can overturn the pellet being captured in front of it and causing enhanced pellet shielding and some plasma pre-cooling there.
The additional plasma loss caused by ELM triggering during LFS pellet injection is also significantly reduced with HFS injection since the pellet material is deposited closer to the plasma core. This causes a more moderate increase of the average radial edge pressure, and the ELM, if it nevertheless occurs, involves less pellet material. A possible benefit may also result from the asymmetric structure of ideal ballooning modes, which are assumed to be involved in type-I ELMs.
In the experiments described slow $D_2$ pellets of 130 m/s are injected into type-I ELMy H-mode plasma as well from the LFS as from the HFS of ASDEX Upgrade. We observed a deeper penetration for injection from the HFS compared to injection from the LFS by more than a factor of 2. The fuelling efficiency for the HFS injection is enhanced dramatically by a factor of more than about 4 without deterioration of plasma confinement. No significant power degradation of the fuelling efficiency is observed for HFS pellet injection. Observations made supports the idea of a toroidal drift of a high-ß plasmoid forced by the plasma.
Thus, because of obvious advantage, HFS pellet injection should be considered as the prime candidate for plasma refuelling in next generation fusion experiments despite the worse accessibility. From the basic mechanisms involved, we conclude that the favourable features should be retained to a large extent as long as the toroidal force points locally into the hot plasma, thus relaxing the design restrictions a lot.

## REFERENCES


[1] ITER Central Team, Plasma Phys. Control. Fusion **35**, B23 (1996).
[2] S.L. Milora, W.A. Houlberg, L.L. Lengyel, and V. Mertens, Nucl. Fusion **35**, 657 (1995).
[3] C. Andelfinger et al., Rev. Sci. Instrum. 64 (1993) 983.
[4] G. Neu et al., Fusion Technology (Proc. 18th Symp. Karlsruhe, 1994), Vol. 1, Elsevier Science, Amsterdam (1995) 675.
[5] M. Kaufmann et al., Plasma Phys. Control. Fusion,
Vol. 35 Suppl. (12)B, (1993) 205.
[6] F. Ryter et al., in Controlled Fusion and Plasma Physics (Proc. 21th Eur. Conf. Montpellier, 1994), Vol. 18B, Part I, European Physical Society, Geneva (1994) 330.
[7] S.L. Milora, J. Fusion Energy 1 (1981) 15.
[8] C.T. Chang and K. Thomsen, Nucl. Fusion 24 (1984) 697.
[9] M. Kaufmann et al., Nucl. Fusion 28 (1988) 827.
[10] G.L. Schmidt et al., in Plasma Physics and Controlled Nuclear Fusion Research 1984 (Proc. 10th Int. Conf. London, 1984), Vol. 1,
IAEA, Vienna (1985) 45.
[11] P.K. Mioduszewski et al., in Plasma Physics and Controlled Nuclear Fusion Research 1984 (Proc. 10th Int. Conf. London, 1984), Vol. 1,
IAEA, Vienna (1985) 257.
[12] R.J. Fonck et al., J. Nucl. Mater. 128&129 (1984) 330.
[13] A. Carlson et al., in Controlled Fusion and Plasma Heating (Proc. 15th Eur. Conf. Dubrovnik, 1988), Vol. 12B, Part III,
European Physical Society, Geneva (1988) 1069.
[14] D.K. Owens et al., in Controlled Fusion and Pellet Injection and Toroidal Confinement (Proc. Tech. Comm. Mtg., Gut Ising, 1988),
IAEA-TECDOC-534, IAEA, Vienna (1989) 191.
[15] H.W. Drawin and A. Géraud, Nucl. Fusion 29 (1989) 1681.
[16] L.R. Baylor et al., Nucl. Fusion 32 (1992) 2177.
[17] P.T. Lang et al., Nucl. Fusion, in press; Rep. IPP 1/296, Max-Planck-Institut für Plasmaphysik, Garching (1996).
[18] N. Greenwald et al., Nucl. Fusion 28 (1988) 2199.
[19] O. Kardaun (H-Mode Database Working Group) in Plasma Physics and Controlled Nuclear Fusion Research 1992 (Proc. 14th Int. Conf. Würzburg, 1992), Vol. 3,
IAEA, Vienna (1993) 251.
[20] C.A. Foster et al., Nucl. Fusion **17**, 1067 (1977).
[21] K. Büchl, G.C. Vlases, W. Sandmann, and R.S. Lang, Nucl. Fusion **27**, 1939 (1987).
[22] L.R. Baylor et al., Nucl. Fusion, in press.
[23] L.L. Lengyel, Phys. Fluids **31**, 1577 (1988).

[24] L.L. Lengyel, Nucl. Fusion **17**, 805 (1977).
[25] M. Kaufmann, K. Lackner, L. Lengyel, and W. Schneider, Nucl. Fusion **26**, 171 (1986).
[26] R.D. Durst et al., Nucl. Fusion **30**, 3 (1990).